

Magnetic and electronic properties of bulk and two-dimensional $FeBi_2Te_4$: A first-principles study

Qianqian Wang(王倩倩), Jianzhou Zhao(赵建洲), Weikang Wu(吴维康), Yinning Zhou(周胤宁), Qile Li, Mark T. Edmonds, and Shengyuan A. Yang(杨声远)

Citation: Chin. Phys. B, 2023, 32 (**8**): 087506. DOI: 10.1088/1674-1056/acd522
Journal homepage: http://cpb.iphy.ac.cn; http://iopscience.iop.org/cpb

What follows is a list of articles you may be interested in

Prediction of a monolayer spin-spiral semiconductor: CoO with a honeycomb lattice

Jie Zhang(张杰), Shunuo Song(宋姝诺), Yan-Fang Zhang(张艳芳), Yu-Yang Zhang(张余洋), Sokrates T. Pantelides, and Shixuan Du(杜世萱)
Chin. Phys. B, 2023, 32 (**8**): 087508. DOI: 10.1088/1674-1056/acd923

Prediction of $LiCrTe_2$ monolayer as a half-metallic ferromagnet with a high Curie temperature

Li-Man Xiao(肖丽蔓), Huan-Cheng Yang(杨焕成), and Zhong-Yi Lu(卢仲毅)
Chin. Phys. B, 2023, 32 (**5**): 057505. DOI: 10.1088/1674-1056/acbe2e

Incommensurate-commensurate magnetic phase transition in double tungstate $Li_2Co(WO_4)_2$

Xiyu Chen(陈西煜), Ning Ding(丁宁), Meifeng Liu(刘美风), Tao Zou(邹涛), V. Ovidiu Garlea, Jingwen Gong(龚婧雯), Fei Liu(刘飞), Yunlong Xie(谢云龙), Lun Yang(杨伦), Shuhan Zheng(郑书翰), Xiuzhang Wang(王秀章), Shuai Dong(董帅), T. Charlton, and Jun-Ming Liu(刘俊明)
Chin. Phys. B, 2022, 31 (**4**): 047501. DOI: 10.1088/1674-1056/ac3818

Magnetic anisotropy in 5d transition metal-porphyrin molecules

Yan-Wen Zhang(张岩文), Gui-Xian Ge(葛桂贤), Hai-Bin Sun(孙海斌), Jue-Ming Yang(杨觉明), Hong-Xia Yan(闫红霞), Long Zhou(周龙), Jian-Guo Wan(万建国), and Guang-Hou Wang(王广厚)
Chin. Phys. B, 2021, 30 (**4**): 047501. DOI: 10.1088/1674-1056/abcf9c

Magnetic phase diagram of single-layer $CrBr_3$

Wei Jiang(江伟), Yue-Fei Hou(侯跃飞), Shujing Li(李淑静), Zhen-Guo Fu(付振国), and Ping Zhang(张平)
Chin. Phys. B, 2021, 30 (**12**): 127501. DOI: 10.1088/1674-1056/ac0043

Magnetic and electronic properties of bulk and two-dimensional $FeBi_2Te_4$: A first-principles study

Qianqian Wang(王倩倩)[1], Jianzhou Zhao(赵建洲)[2,1,†], Weikang Wu(吴维康)[3,1‡], Yinning Zhou(周胤宁)[4], Qile Li[5,6], Mark T. Edmonds[5,6], and Shengyuan A. Yang(杨声远)[1]

[1] *Research Laboratory for Quantum Materials, Singapore University of Technology and Design, Singapore* 487372, *Singapore*

[2] *Co-Innovation Center for New Energetic Materials, Southwest University of Science and Technology, Mianyang* 621010, *China*

[3] *Key Laboratory for Liquid–Solid Structural Evolution and Processing of Materials (Ministry of Education), Shandong University, Jinan* 250061, *China*

[4] *Joint Key Laboratory of the Ministry of Education, Institute of Applied Physics Materials Engineering, University of Macau, Macau Special Administrative Region, China*

[5] *School of Physics and Astronomy, Monash University, Clayton, VIC* 3800, *Australia*

[6] *ARC Centre for Future Low Energy Electronics Technologies, Monash University, Clayton, VIC* 3800, *Australia*

(Received 6 February 2023; revised manuscript received 10 May 2023; accepted manuscript online 12 May 2023)

Layered magnetic materials, such as $MnBi_2Te_4$, have drawn much attention owing to their potential for realizing two-dimensional (2D) magnetism and possible topological states. Recently, $FeBi_2Te_4$, which is isostructural to $MnBi_2Te_4$, has been synthesized in experiments, but its detailed magnetic ordering and band topology have not been clearly understood yet. Here, based on first-principles calculations, we investigate the magnetic and electronic properties of $FeBi_2Te_4$ in bulk and 2D forms. We show that different from $MnBi_2Te_4$, the magnetic ground states of bulk, single-layer, and bilayer $FeBi_2Te_4$ all favor a 120° noncollinear antiferromagnetic ordering, and they are topologically trivial narrow-gap semiconductors. For the bilayer case, we find that a quantum anomalous Hall effect with a unit Chern number is realized in the ferromagnetic state, which may be achieved in experiment by an external magnetic field or by magnetic proximity coupling. Our work clarifies the physical properties of the new material system of $FeBi_2Te_4$ and reveals it as a potential platform for studying magnetic frustration down to 2D limit as well as quantum anomalous Hall effect.

Keywords: $FeBi_2Te_4$, two-dimensional (2D) magnetism, noncollinear antiferromagnet, quantum anomalous Hall effect, first-principles calculation

PACS: 75.50.Ee, 73.43.–f, 31.15.A–, 74.20.Pq **DOI:** 10.1088/1674-1056/acd522

1. Introduction

Magnetism and magnetic materials have always been a major subject in condensed matter physics research. There are recently two emerging directions in this field. One is to push magnetism into two-dimensional (2D) systems. Several 2D magnetic materials have been realized experimentally[1–3] and more have been predicted.[4,5] Here, a commonly used approach is to start from an existing bulk magnetic material which has a layered structure bonded by the weak van der Waals (vdW) interaction, such that 2D layers can be fabricated via mechanical exfoliation. The other direction is to explore magnetic topological states.[6,7] Certain topological states, such as the famous quantum anomalous Hall (QAH) insulator,[8–10] must require magnetism. The interplay between magnetic ordering and band topology is expected to enable novel spintronic devices.[11–13]

Previous studies revealed $MnBi_2Te_4$ as an interesting magnetic material system,[14–18] which is actually at the merging point of the two directions. On one hand, it is a vdW layered magnetic material in the bulk, which can be readily thinned down to 2D layers. On the other hand, bulk $MnBi_2Te_4$ realizes an antiferromagnetic (AFM) topological insulator, and in 2D form, it can exhibit QAH state, zero plateau QAH state or axion insulator state, depending on the number of layers.[14–16] Other Mn-based ternary compounds in the same family, such as $MnBi_2Se_4$ and $MnSb_2Te_4$,[19,20] were also investigated and found nontrivial properties.

In a recent experiment, Saxena *et al.*[21] reported the successful synthesis of the bulk $FeBi_2Te_4$ single crystals, which adopts the same vdW layered structure as $MnBi_2Te_4$. Magnetic measurement showed that the material has an AFM ground state, and there seemed to be a transition to ferromagnetic (FM) or ferrimagnetic state at ~ 250 K.[21] Due to the similarity between structures of $FeBi_2Te_4$ and $MnBi_2Te_4$, it was strongly suggested that $FeBi_2Te_4$ may also realize topologically nontrivial states in the bulk or 2D forms. Nevertheless, so far, the detailed magnetic ordering, which is a prerequisite for determining the band topology, has not been clarified yet.

In this work, we systematically investigate the magnetic and electronic properties of $FeBi_2Te_4$ by using first-principles

†Corresponding author. E-mail: jzzhao@swust.edu.cn
‡Corresponding author. E-mail: weikang_wu@sdu.edu.cn

© 2023 Chinese Physical Society and IOP Publishing Ltd

calculations. We find that in the bulk form, different from $MnBi_2Te_4$, the ground state of $FeBi_2Te_4$ favors an AFM state with a 120° non-collinear ordering within each Fe plane. Its band structure is a semiconductor with a direct band gap about 0.25 eV. We further study 2D $FeBi_2Te_4$ structures, including one septuple layer (1-SL) and 2-SL $FeBi_2Te_4$. We show that they both prefer the intralayer 120° AFM ordering and are narrow-gap semiconductors. Although their ground states are topologically trivial, the FM state of 2-SL $FeBi_2Te_4$, which may be achieved by the applied field or proximity effect, is found to be a QAH insulator with a unit Chern number and a band gap of 0.06 eV. Our result suggests an interesting frustrated magnetic ordering in bulk and 2D $FeBi_2Te_4$, and provides useful guidance for the study of electronic properties of this new magnetic system.

2. Computation method

Our first-principles calculations were carried out by using the Vienna *ab initio* simulation package (VASP),[22,23] which is based on the density functional theory. The projector augmented wave method[24] was used to treat the ionic potentials, with a kinetic energy cutoff of 450 eV. The exchange–correlation energy was treated using the Perdew–Burke–Ernzerhof (PBE) approach.[25] Correlation effects for Fe 3d orbitals were treated by the PBE plus Hubbard U (PBE+U) method,[26,27] with $U = 4$ eV for both structural relaxation and electronic calculation.[28,29] We have also tested U values from 3 eV to 5 eV and found no qualitative change in the major results. The spin–orbit coupling (SOC) is fully considered in our calculation. The vdW interaction was included by the DFT-D3 approach.[30] The convergence criteria for the energy and for the atomic force were set to be 10^{-6} eV and 10^{-2} eV/Å, respectively. The different magnetic orderings affect the size of unit cell, which in turn affects the Brillouin zone (BZ) size. Accordingly, the size of k-mesh needed for BZ sampling also changes. For bulk $FeBi_2Te_4$, a $5\times5\times5$ Monkhorst–Pack k-mesh[31] was used for nonmagnetic and FM states, a $3\times3\times3$ k-mesh for AFM-I state and a $5\times5\times1$ k-mesh for the AFM-II state for the BZ integration. For 2D $FeBi_2Te_4$ lattices, a $9\times9\times1$ k-mesh was used for nonmagnetic and FM states, a $5\times9\times1$ k-mesh for the striped AFM state and a $5\times5\times1$ k-mesh for AFM-II state. For 2D calculations, a vacuum space of 18-Å thickness is added to minimize the interaction between periodic images. The wannier band is calculated with a tight-binding (TB) model based on the maximally localized Wannier functions (MLWFs), as implemented in the Wannier90 code.[32] The topological properties and edge spectrum were calculated by using the WannierTools package.[33]

3. Results and discussion

3.1. Bulk property

Let us first study bulk $FeBi_2Te_4$. It is a vdW layered material with the same type of lattice structure as $MnBi_2Te_4$. As illustrated in Fig. 1, each $FeBi_2Te_4$ layer consists of seven atomic layers (each layer forms a triangular lattice), stacked in the sequence of Te–Bi–Te–Fe–Te–Bi–Te. And these $FeBi_2Te_4$ layers are stacked in the *ABC*-type manner. The space group for the lattice is $R\bar{3}m$. The experimentally determined lattice constants are $a = 4.3926$ Å and $c = 42.6944$ Å.[21] We adopt these values in our first-principles calculation.

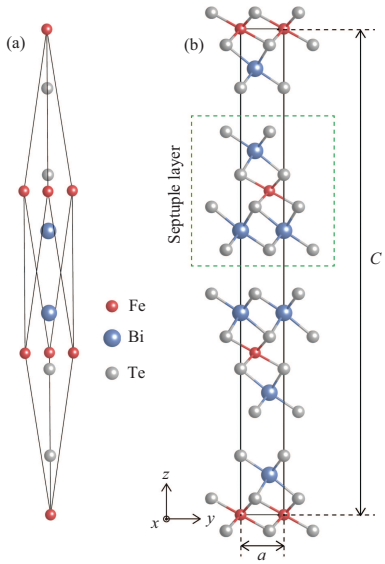


Fig. 1. (a) Primitive cell and (b) conventional cell of bulk $FeBi_2Te_4$.

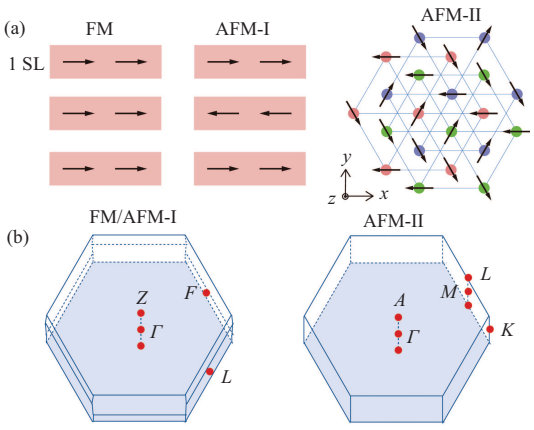


Fig. 2. (a) Illustration of FM, AFM-I, and AFM-II magnetic orderings of bulk $FeBi_2Te_4$. For AFM-II, the Fe sites in three neighboring layers (*ABC*) are marked by three different colors. (b) Brillouin zones for FM/AFM-I state (left) and for AFM-II state (right).

Like $MnBi_2Te_4$, the magnetism is mainly from the sites with 3d magnetic ions, which is Fe here. In Ref. [21], the ground state was found to be AFM but the detailed configuration was not determined. To figure out the magnetic configuration, we investigate the energetics for several configurations as shown in Fig. 2(a). Specifically, we compare energies for nonmagnetic (NM), FM, and AFM states. For AFM, we consider

two types of states. One is the collinear AFM in Fig. 2(a), labeled as AFM-I where each Fe layer is FM ordered and two neighboring Fe layers are AFM coupled. The other state is the 120° AFM order in Fig. 2(a), labeled as AFM-II, where within each Fe layer, each local spin lies in the layer plane and makes an 120° angle with its neighboring spins. This is a typical frustrated magnetic configuration on hexagonal lattices. SOC is included in our calculations. For the FM and AFM states, we also consider several spin orientations to find the preferred direction. Our calculation results are listed in Table 1.

We have the following observations from Table 1. First, the energy for the nonmagnetic state is much higher than that of the magnetic states, this indicates the magnetic ordering in the ground state of $FeBi_2Te_4$. Second, among the magnetic states, the 120° AFM state is found to possess the lowest energy. This shows that the bulk $FeBi_2Te_4$ is an interesting vdW material with frustrated magnetic ordering. This is consistent with the experimental report of an AFM state. Third, the result shows that the local spins prefer to lie within the layer plane rather than out of plane. For FM, AFM-I, and AFM-II states, we also tested different in-plane orientations for local spins and found that the energy difference is negligible.

Next, we investigate the electronic band structures for some representatives in Table 1, including NM, FM_x, $AFM\text{-}I_x$, and AFM-II states. The results are plotted in Fig. 3. One can see that all these states are semiconductors. Their energy gaps are 0.20 eV for NM, 0.25 eV for FM_x, 0.29 eV for $AFM\text{-}I_x$, and 0.25 eV for AFM-II state. It was reported that bulk $MnBi_2Te_4$ is an AFM topological insulator. Here, we check the band topologies for the states in Fig. 3 and find that they are topologically trivial.

Table 1. Relatively energy ΔE (in units meV/f.u.) measured from the ground state (AFM-II), magnetic space group (MSG), and band gap (in unit eV) for NM, FM, AFM-I, and AFM-II orderings in bulk $FeBi_2Te_4$.

	NM	FM_x	$AFM\text{-}I_x$	AFM-II
ΔE	2125.59	19.26	16.77	0
MSG	$R\bar{3}m1'$	$C2/m$	C_c2/m	Cm
Band gap	0.20	0.25	0.29	0.25

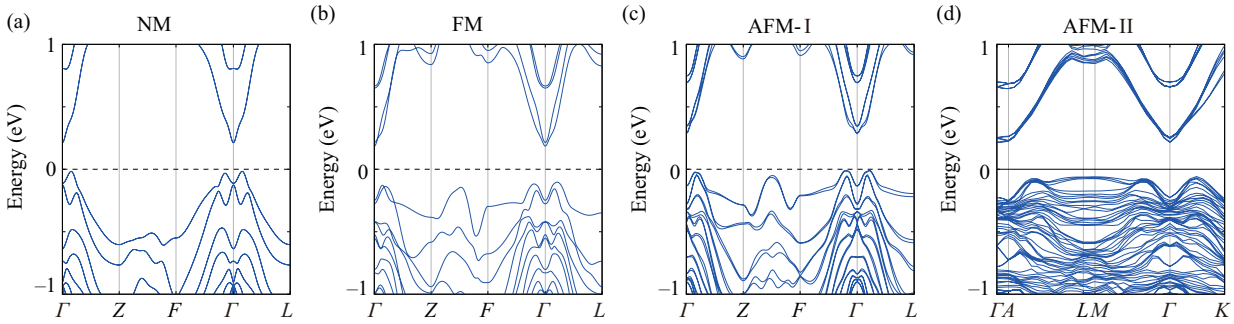


Fig. 3. Band structures of bulk $FeBi_2Te_4$ with different magnetic orderings: (a) NM, (b) FM, (c) AFM-I, and (d) AFM-II.

3.2. Single layer property

Since bulk $FeBi_2Te_4$ is a vdW layered material, its 2D ultrathin layers can be obtained by using exfoliation method. In this section, we study the properties of single-layer $FeBi_2Te_4$, see Fig. 4. After structural relaxation, we find that the isolated 1-SL does not change much from a layer in the bulk. The lattice space group is $P\bar{3}m1$. The optimized lattice constant is $a = 4.32$ Å, and the thickness t is 10.73 Å.

To determine the magnetic ground state for 1-SL $FeBi_2Te_4$, we consider the magnetic configurations as shown in Fig. 4(c). Here, FM and AFM-II are configurations similar to the bulk case. We also consider an additional stripe AFM (AFM-S) configuration in Fig. 4(c). Again, for each case, we have tested different orientations of the spins. The calculated energies are listed in Table 2.

The result shows that the frustrated 120° AFM remains to be the ground state in the single layer limit. This is distinct from 1-SL $MnBi_2Te_4$[16,18,34,35] and other existing two-dimensional magnets, such as Fe_3GeTe_2 and CrI_3.[36,37] Those two-dimensional materials have either FM or collinear AFM ordering.

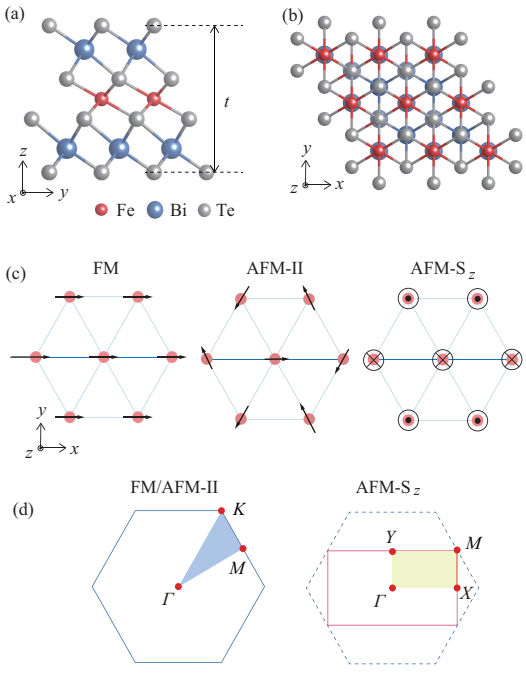


Fig. 4. (a) Side view and (b) top view of 1-SL $FeBi_2Te_4$. (c) Illustration of FM, AFM-II, and AFM-S_z magnetic orderings in 1-SL $FeBi_2Te_4$. (d) Brillouin zones for FM and AFM-II states (left) and for AFM-S_z state (right).

Table 2. Relatively energy ΔE (in units meV/f.u.) measured from the ground state (AFM-II), magnetic space group (MSG), and band gap (in unit eV) for NM, FM, AFM-I, and AFM-II orderings in 1-SL $FeBi_2Te_4$.

	NM	FM_x	AFM-S_z	AFM-II
ΔE	2168.80	45.03	4.75	0
MSG	$P\bar{3}m11'$	$C2/m$	C_c2/m	Cm
Band gap	0.30	0.28	0.4	0.37

The calculated band structures for these states are plotted in Fig. 5. One observes that all these states are semiconductors. The band gaps are 0.30 eV for NM, 0.28 eV for FM, 0.40 eV for AFM-S, and 0.37 eV for AFM-II state, respectively. The band gaps about 0.3 eV to 0.4 eV make these materials new candidates as 2D narrow-gap semiconductors, which could be useful for infrared detection.

For 2D magnetic materials, an intriguing possibility is the realization of QAH insulator state. A QAH insulator is characterized by a nontrivial Chern number for its bulk band structure and features chiral edge modes. We have computed the Chern numbers for the band structures in Fig. 5 and found that they are all trivial.

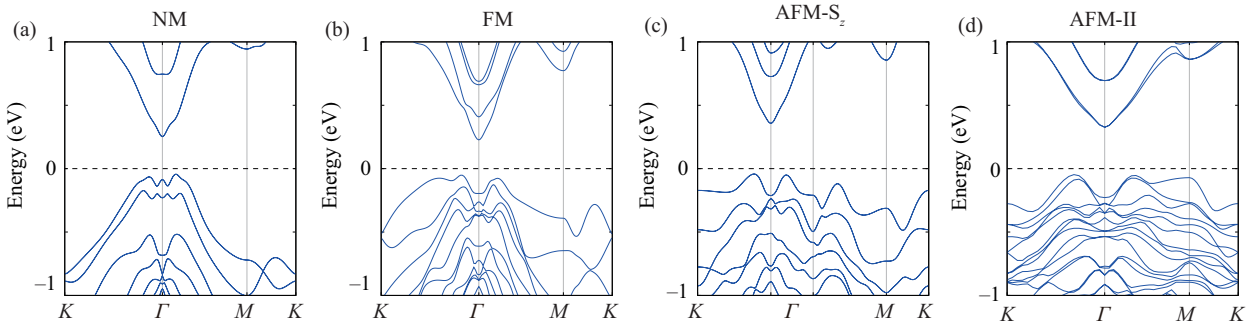


Fig. 5. Band structures of 1-SL $FeBi_2Te_4$ with different magnetic orderings: (a) NM, (b) FM, (c) AFM-S_z, and (d) AFM-II.

3.3. Bilayer property

Next, we turn our attention to 2-SL $FeBi_2Te_4$. As shown in Fig. 6(a), 2-SL $FeBi_2Te_4$ has a space group of $P\bar{3}m1$. The optimized lattice constant is given by $a = 4.31$ Å, and the thickness t is 24.01 Å.

We compare the magnetic configurations as shown in Fig. 6(b). These include NM, FM, AFM-I, and AFM-II. Here, we use red and green colors to mark the Fe atoms in different septuple layers. The calculated energies are presented in Table 3. We find that the ground state is still the frustrated AFM-II state.

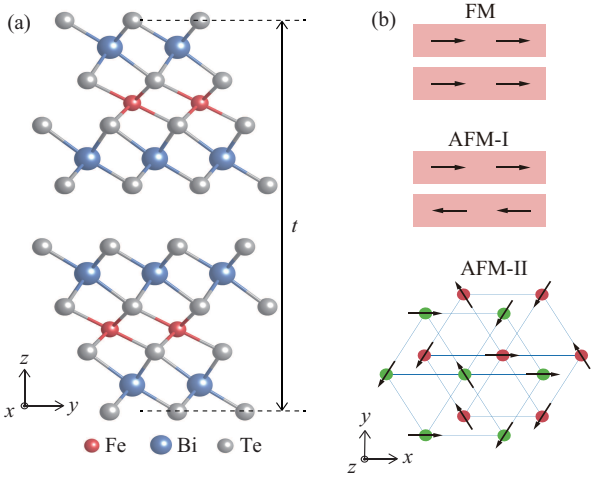


Fig. 6. (a) Side view of 2-SL $FeBi_2Te_4$. (b) Illustration of FM, AFM-I, and AFM-II magnetic orderings in 2-SL $FeBi_2Te_4$. For AFM-II, the Fe sites in different layers are marked by two different colors.

The band structures for 2-SL $FeBi_2Te_4$ with the different magnetic configurations are shown in Fig. 7. One notes that all these states are semiconductors, but their band gaps are smaller compared to both 1-SL and the bulk. The AFM-II ground state only has a band gap about 10 meV.

Table 3. Relatively energy ΔE (in units meV/f.u.) measured from the ground state (AFM-II), magnetic space group (MSG), and band gap (in unit eV) for NM, FM, AFM-I, and AFM-II orderings in 2-SL $FeBi_2Te_4$.

	NM	FM_x	AFM_x	AFM-II
ΔE	2051.42	7.96	5.50	0
MSG	$P\bar{3}m11'$	$C2/m$	$C2'/m$	$P\bar{3}1m$
Band gap	0.10	0.06	0.08	0.01

Relatively energy ΔE (in units meV/f.u.) To check possible nontrivial topology in these states, we calculate their Chern numbers by the Wilson loop method.[38] The result shows that the FM state with out-of-plane (z) magnetization, which holds a slight higher relatively energy $\Delta E = 8.25$ meV/f.u., has a nontrivial Chern number $\mathscr{C} = -1$, whereas other states are topologically trivial. In Fig. 8(a), we plot the variation of intrinsic anomalous Hall conductivity σ_{xy} *versus* the chemical potential.[39–42] It is calculated by

$$\sigma_{xy} = \frac{e^2}{\hbar}\sum_n \int_{\mathrm{BZ}} \frac{\mathrm{d}^2k}{(2\pi)^2} f_0(\varepsilon_{n\boldsymbol{k}})\Omega_z^n(\boldsymbol{k}), \tag{1}$$

where f_0 is the Fermi distribution function, $\varepsilon_{n\boldsymbol{k}}$ is the energy for (cell-periodic part of) Bloch state $|u_{n\boldsymbol{k}}\rangle$, and

$$\Omega_z^n(\boldsymbol{k}) = -2\,\mathrm{Im}\langle\partial_{k_x}u_{n\boldsymbol{k}}|\partial_{k_y}u_{n\boldsymbol{k}}\rangle \tag{2}$$

is the Berry curvature for a 2D system. Inside a spectral gap,

σ_{xy} must be quantized as

$$\sigma_{xy} = \frac{e^2}{h}\mathscr{C}, \tag{3}$$

with $\mathscr{C}$ being the Chern number. From Fig. 8(a), one observes that in the band gap (~ 60 meV) of FM_z state, the Hall conductivity indeed takes a constant quantized value of $-e^2/h$, indicating that the system is a QAH insulator.

The unit Chern number indicates that on the edge of the sample, there must be a single gapless chiral edge band. This is explicitly confirmed by our calculated edge spectrum in Fig. 8(b). One can clearly see the presence of one chiral edge band that traverses the bulk band gap.

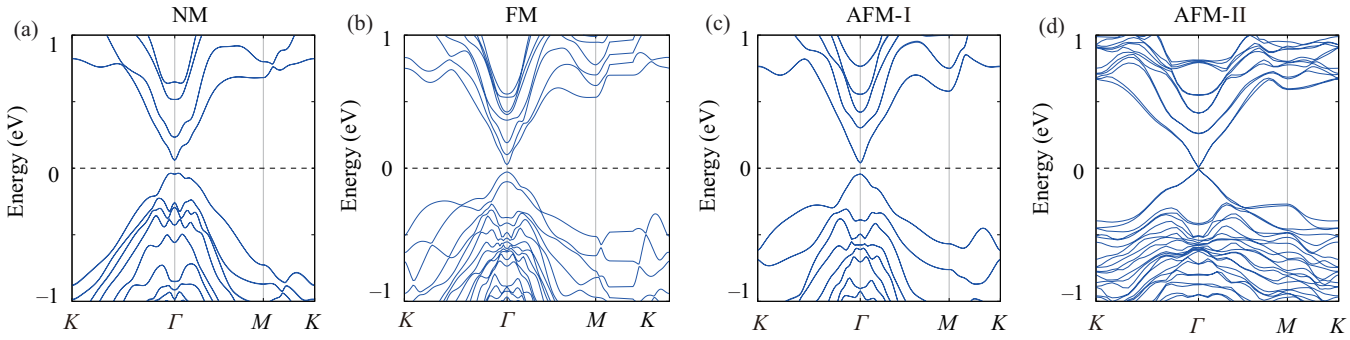


Fig. 7. Band structures of 2-SL $FeBi_2Te_4$ with different magnetic orderings: (a) NM, (b) FM, (c) AFM-I, and (d) AFM-II.

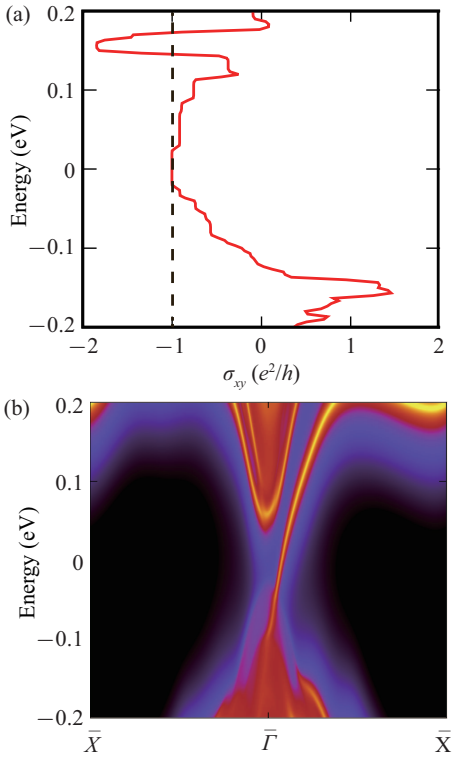


Fig. 8. (a) Intrinsic anomalous Hall conductance σ_{xy} plotted against the chemical potential for 2-SL $FeBi_2Te_4$ in the FM_z state. (b) Edge spectrum for the (010) edge, which shows one gapless chiral edge band.

Although FM_z state is not the ground state of 2-SL $FeBi_2Te_4$, in practice, it may be realized by applying an external B field along the z direction or by exchange coupling to nearby magnetic materials, given that 2D materials are much more tunable than 3D materials. Actually, the similar mechanism to change magnetic configuration from AFM to FM was recently demonstrated in 2D CrI_3.[43] And magnetic proximity coupling in vdW heterostructures were also demonstrate in a number of systems.[2,44–46]

4. Discussion and conclusion

In this work, we find that both bulk and 2D $FeBi_2Te_4$ favor a noncollinear AFM ground state. This is a quite interesting result and contrasts with the behavior in $MnBi_2Te_4$. To understand this, we note the following points. First, triangular lattice is a well-known lattice with geometric frustration, the 120° noncollinear AFM order is a natural ordering on this lattice. Second, there is no inversion center between two neighboring Fe sites, so it allows a Dzyaloshinskii–Moriya (DM)-type interaction from SOC between two neighboring moments. It is known that DM interaction tends to favor noncollinear configuration. Since Fe has stronger SOC than Mn (due to its larger atomic number), one expects that this DM interaction strength is also larger. (We have tested that the noncollinear AFM order in $FeBi_2Te_4$ is quite robust against lattice strains and applied electric fields.) In addition, we mention that the electronic correlation plays an important role here. We find that with $U = 0$, the system is in fact metallic. This implies that the insulating behavior here is likely of Mott type. To have better understanding of correlation effects in this system, more advanced treatments should be taken in future studies.

Finally, it is known that DM interaction and noncollinear magnetism can give rise to magnetic textures such as skyrmions. A recent work by Cui *et al.*[47] predicted interesting skyrmion structures in vdW AFM materials $MnBi_2Se_2Te_2$ bilayers and trilayers. Based on the above discussion, similar physics may also appear in $FeBi_2Se_2Te_2$, which is an interesting topic to explore in future works.

In conclusion, we have systematically studied the magnetic and electronic properties of a newly synthesized material $FeBi_2Te_4$. Interestingly, we find that although $FeBi_2Te_4$

has the same lattice structure as $MnBi_2Te_4$, they have different magnetic ground states. In $MnBi_2Te_4$, the magnetic configurations are collinear, but $FeBi_2Te_4$ in both bulk and 2D forms, tends to adopt a noncollinear frustrated AFM configurations. This offers a new platform to study frustrated magnetism, which is still rare among 2D materials studied so far. Electronically, $FeBi_2Te_4$ are found to be narrow-gap semiconductors. In ground states, the gap value is 0.25 eV for the bulk and shows a strong variation from 1-SL to 2-SL. Again, different from $MnBi_2Te_4$ which possess a variety of magnetic topological phases, most states of $FeBi_2Te_4$ are found to be trivial. Nevertheless, in 2-SL $FeBi_2Te_4$, we show that the FM_z state is QAH insulator with a unit Chern number, which may be achieved in experiment by an applied magnetic field or by magnetic proximity coupling. Our work clarifies important physical properties of the new material $FeBi_2Te_4$ and will be useful for guiding subsequent experimental studies.

Acknowledgments

The authors thank H. Wang and W. J. Huang for helpful discussions. We acknowledge the funding support from the Singapore MOE AcRF 308 Tier 2 (Grant No. T2EP50220-0026). W. Wu acknowledges the funding support from Shandong Provincial Natural Science Foundation (Grant No. ZR2023QA012), and the Special Funding in the Project of Qilu Young Scholar Program of Shandong University. M. T. Edmonds acknowledges the funding support from Australian Research Council Future Fellowship (Grant No. FT220100290). Q. Li acknowledges the funding support from the AINSE postgraduate award. Y. Zhou acknowledges the funding support from the Research and Development Administration Office at the University of Macau (Grants Nos. MYRG2022-00088-IAPME and SRG2021-00003-IAPME).

Appendix A: Comparison of properties between $FeBi_2Te_4$ and $MnBi_2Te_4$

$FeBi_2Te_4$ and $MnBi_2Te_4$ are isostructural materials. However, their ground state magnetic orderings are different, which leads to different magnetic space group symmetries and different topological classifications. $MnBi_2Te_4$ was found to have a collinear AFM ordering with an important $S = \Theta T_{1/2}$ symmetry, where Θ is time inversion and $T_{1/2}$ is a factional lattice translation connecting adjacent septuple layers.[14] This symmetry protects the AFM topological insulator state in $MnBi_2Te_4$. In comparison, $FeBi_2Te_4$ takes noncollinear AFM-II ordering, which does not have the S symmetry. Thus, it cannot realize the AFM topological insulator state as $MnBi_2Te_4$. In Table A1, we list the different properties for $FeBi_2Te_4$ and $MnBi_2Te_4$ and also for their 2D layers.

Table A1. Comparison of properties for $FeBi_2Te_4$ and $MnBi_2Te_4$.

	$FeBi_2Te_4$			$MnBi_2Te_4$ (Refs. [14,16])		
	Bulk	1-SL	2-SL	Bulk	1-SL	2-SL
Magentic state	AFM-II	AFM-II	AFM-II	AFM_z	FM_z	AFM_z
Magnetic moment (μ_B)	3.566	3.571	3.548	4.6	4.6	4.6
Topology	Trivial	Trivial	Trivial	TI	Trivial	QAH AI[a]

[a]AI: axion insulator.

References

[1] Deng Y, Yu Y, Song Y, *et al.* 2018 *Nature* **563** 94
[2] Gong C, Li L, Li Z, *et al.* 2017 *Nature* **546** 265
[3] Huang B, Clark G and Navarro-Moratalla E 2017 *Nature* **546** 270
[4] Lu S, Zhou Q, Guo Y, Zhang Y, Wu Y and Wang J 2020 *Adv. Mater.* **32** 2002658
[5] Mounet N, Gibertini M, Schwaller P, *et al.* 2018 *Nature Nanotechnol.* **13** 246
[6] Bernevig B A, Felser C and Beidenkopf H 2022 *Nature* **603** 41
[7] Tokura Y, Yasuda K and Tsukazaki A 2019 *Nat. Rev. Phys.* **1** 126
[8] Yu R, Zhang W, Zhang H J, Zhang Shou C, Dai X and Fang Z 2010 *Science* **329** 61
[9] Chang C Z, Zhang J, Feng X, *et al.* 2013 *Science* **340** 167
[10] Duncan F and Haldane M 1988 *Phys. Rev. Lett.* **61** 2015
[11] Pesin D and MacDonald A H 2012 *Nat. Mater.* **11** 409
[12] Šmejkal L, Mokrousov Y, Yan B and MacDonald A H 2018 *Nat. Phys.* **14** 242
[13] Li P, Wu W, Wen Y, Zhang C, Zhang J, Zhang S, Yu Z, Yang S A, Manchon A and Zhang X 2018 *Nat. Commun.* **9** 3990
[14] Li J, Li Y, Du S, Wang Z, Gu B L, Zhang S C, He K, Duan W and Xu Y 2019 *Sci. Adv.* **5** eaaw5685
[15] Zhang D, Shi M, Zhu T, Xing D, Zhang H and Wang J 2019 *Phys. Rev. Lett.* **122** 206401
[16] Otrokov M M, Rusinov Igor P, Blanco-Rey M, Hoffmann M, Yu V A, Eremeev S V, Ernst A, Echenique P M, Arnau A and Chulkov E V 2019 *Phys. Rev. Lett.* **122** 107202
[17] Otrokov M M, Klimovskikh I I, Bentmann H, *et al.* 2019 *Nature* **576** 416
[18] Deng Y, Yu Y, Shi M Z, Guo Z, Xu Z, Wang J, Chen X H and Zhang Y 2020 *Science* **367** 895
[19] Zhu T, Bishop A J, Zhou T, *et al.* 2021 *Nano Lett.* **21** 5083
[20] Zhou L, Tan Z, Yan D, Fang Z, Shi Y and Weng H 2020 *Phys. Rev. B* **102** 085114
[21] Saxena A, Rani P, Nagpal V, Patnaik S, Felner I and Awana V P S 2020 *Journal of Superconductivity and Novel Magnetism* **33** 2251
[22] Kresse G and Hafner J 1993 *Phys. Rev. B* **47** 558
[23] Kresse G and Joubert D 1999 *Phys. Rev. B* **59** 1758
[24] Blöchl P E 1994 *Phys. Rev. B* **50** 17953
[25] Perdew J P, Burke K and Ernzerhof M 1996 *Phys. Rev. Lett.* **77** 3865
[26] Anisimov V I, Zaanen J and Andersen O K 1991 *Phys. Rev. B* **44** 943
[27] Dudarev S L, Botton G A, Savrasov S Y, Humphreys C J and Sutton A P 1998 *Phys. Rev. B* **57** 1505

[28] Rollmann G, Rohrbach A, Entel P and Hafner J 2004 *Phys. Rev. B* **69** 165107
[29] Kulik H J, Cococcioni M, Scherlis D A and Marzari N 2006 *Phys. Rev. Lett.* **97** 103001
[30] Stefan G, Antony J, Ehrlich S and Krieg H 2010 *J. Chem. Phys.* **132** 154104
[31] Monkhorst H J and Pack J D 1976 *Phys. Rev. B* **13** 5188
[32] Mostof A A, Yates J R, Pizzi G, Lee Y S, Souza I, Vanderbilt D and Marzari N 2014 *Comput. Phys. Commun.* **185** 2309
[33] Wu Q, Zhang S N, Song H F, Troyer M and Soluyanov A A 2018 *Comput. Phys. Commun.* **224** 405
[34] Yang S, Xu X, Zhu Y, *et al.* 2021 *Phys. Rev. X* **11** 011003
[35] You J Y, Dong X J, Gu B and Su G 2021 *Phys. Rev. B* **103** 104403
[36] Fei Z, Huang B, Malinowski P, *et al.* 2018 *Nat. Mater.* **17** 778
[37] Huang B, Clark G, Klein D R, *et al.* 2018 *Nat. Nanotechnol.* **13** 544
[38] Yu R, Qi X L, Bernevig A, Fang Z and Dai X 2011 *Phys. Rev. B* **84** 075119
[39] Jungwirth T, Niu Q and MacDonald A H 2002 *Phys. Rev. Lett.* **88** 207208
[40] Yao Y, Kleinman L, MacDonald A H, Sinova J, Jungwirth T, Wang D S, Wang E and Niu Q 2004 *Phys. Rev. Lett.* **92** 037204
[41] Nagaosa N, Sinova J, Onoda S, MacDonald A H and Ong N P 2010 *Rev. Mod. Phys.* **82** 1539
[42] Onoda M and Nagaosa N 2002 *J. Phys. Soc. Jpn.* **71** 19
[43] Song T, Cai X, Tu W Y, *et al.* 2018 *Science* **360** 1214
[44] Li Q, Trang C X, Wu W, Hwang J, Cortie D, Medhekar N, Mo S K, Yang S A and Edmonds M T 2022 *Adv. Mater.* **34** 2107520
[45] Webster L and Yan J A 2018 *Phys. Rev. B* **98** 144411
[46] Li Y, Jiang Z, Li J, Xu S and Duan W 2019 *Phys. Rev. B* **100** 134438
[47] Cui Q, Zhu Y, Liang J, Cui P and Yang H 2023 *Phys. Rev. B* **107** 064422